$\sigma(\gamma,p)/\sigma(\gamma,n)$ ratio, current conservation, and nucleon scattering in ^{4}He

Dean Halderson
Department of Physics, Western Michigan University, Kalamazoo, Michigan 49008-5252, USA
(Received 29 March 2004; published 24 September 2004)

A continuum shell model has been constructed which allows inclusion of any nonspurious states of the core nuclei and any nonspurious states of the composite system. The resulting coupled-channels solutions are antisymmetric and translationally invariant. These wave functions can be used to calculate many nuclear phenomena, from capture reactions at astrophysical energies, to knockout reactions at low energies, to nucleon scattering and charge exchange at intermediate energies. The model is used to investigate the ^{4}He$(\gamma,p)^3$H, ^{4}He$(\gamma,n)^3$He, and, ^{3}He$(p,p)^3$He reactions.

DOI: 10.1103/PhysRevC.70.034607 PACS number(s): 21.60.−n, 24.10.−i

I. INTRODUCTION

The need for accurate solutions of nuclear systems with one particle in the continuum are numerous. Elastic, inelastic and charge exchange reactions, capture reactions, and one-nucleon knockout reactions all require these wave functions. Such reactions are often addressed with optical model, distorted wave, or in some cases with resonating group calculations. Each procedure has approximations which may make them inappropriate for describing particular phenomena. The recoil corrected continuum shell model (RCCSM), introduced by Philpott [1], is also a model, and hence provides an approximate solution to the nuclear many-body problem, but it is one in which it is possible to systematically improve the solution by adding additional shell-model configurations.

The first application of the RCCSM was to nucleon scattering from closed shell nuclei. [1] Here the importance of a translationally invariant model was exhibited. The model was extended to $1p$-$1h$ excitations in Refs. [2–7]. Calculations were made for $A=4$, 12, and 16 composite systems. These calculations included many types of reactions, from investigations of polarization-analyzing power differences in (p,n) reactions [4] to $(\pi,\pi' N)$ knockout reactions [2]. Recently the model was extended to include all p-shell nuclei and applied to medium energy nucleon-induced reactions [8] and to low energy ^{7}Be$+p$ elastic scattering [9]. Now the model has been extended by allowing any $A-1$ shell-model core states, as long as they are nonspurious, and any states of the composite system, as long as they are nonspurious, and include them in a calculation with one nucleon in the continuum. The first purpose of the paper is to describe the implementation of this model.

The most successful application of the RCCSM was to the $A=4$ composite system. The M3Y interaction of Ref. [10] amazingly turned out to be the near perfect effective interaction for cores states of the $0s^3$ configuration. Almost all phenomena involving one nucleon in the continuum below 60 MeV were accurately described by this simple model. Apparently, the main ingredients are the correct effective interaction and the translationally invariant solutions. An exception to this agreement occurs when comparing data from reactions involving real or virtual photons. However, in electron scattering many of the data sets are not consistent with each other, and it was difficult to determine exactly when the calculations were not correctly describing the phenomena. After a comparison with virtually all $(e,e'N)$ data, it was concluded in Ref. [6] that agreement with most data is good, except, on average, the transverse convection current is 10–30% too weak at low momentum transfer and in the energy region $E_x=20-40$ MeV, and that the calculated Coulomb multipoles are possibly too strong in that same momentum and energy region. The real photon case is more clear, in that, one is not sorting through many different energies and momentum transfers, but again, different data sets disagree. This disagreement is demonstrated in Figs. 1 and 2. The data for Fig. 1 have been divided into three groups. The data of Refs. [11–15] are classified as high. Of these, only the data of Ref. [11] are plotted as open circles to represent this group. The data of Refs. [16–18] are classified as intermediate. Of these, only the data of Ref. [17] are plotted as dia-

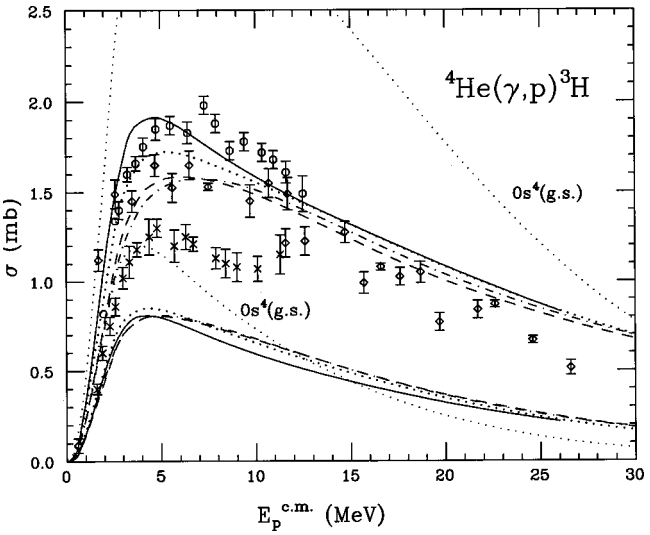

FIG. 1. The ^{4}He$(\gamma,p)^3$H total cross section. The data of Refs. [11, 17, and 19] are plotted as open circles, diamonds, and ×'s, respectively. Light dotted curves are from calculations with $N=0$ with pure $0s^4$ ground state. Solid, dark-dotted, dashes, and dot-dashed lines are for $N=0$, 2, 4, and 6, respectively. Upper curves are with Coulomb operator; lower curves are with transverse current operator.

 ©2004 The American Physical Society

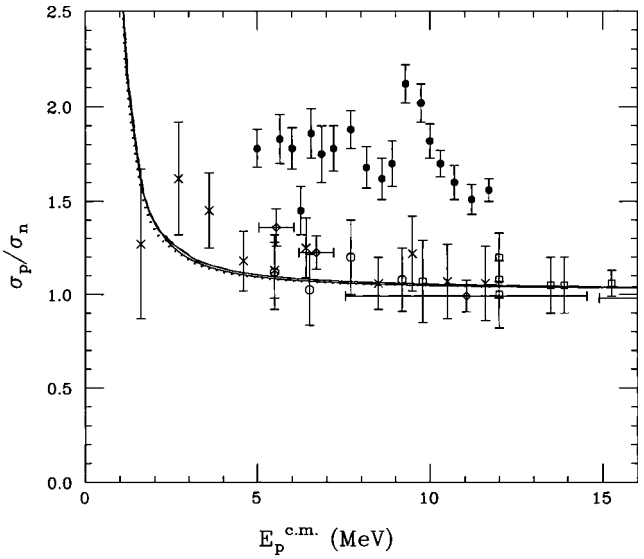

FIG. 2. The ratio $\sigma(\gamma,p)/\sigma(\gamma,n)$. The data of Refs. [13,16,18], [19] divided by [21], and [11] divided by [21] are plotted as open circles, diamonds, open squares, $\times$'s and solid circles, respectively. Curves are the same as in Fig. 1.

monds to represent this group. The data of Refs. [19 and 20] are classified as low. Of these, only the data of Ref. [19] are plotted as $\times$'s to represent this group. Here one sees a 35% discrepancy among data sets in the ^{4}He(γ,p) cross section.

In Fig. 2 the ratio $\sigma(\gamma,p)/\sigma(\gamma,n)$ is plotted for only those data sets that come from the same experiment or the same laboratory, in which both $\sigma(\gamma,n)$ and $\sigma(\gamma,p)$ magnitudes were determined, and that extend into the peak cross section region. Therefore, the data of Refs. [13,16,18], and [19] divided by [21] are plotted as open circles, diamonds, open squares, and $\times$'s, respectively. The data of Ref. [11] divided by that of Ref. [21] are also plotted as solid circles to demonstrate one among the many ways that a ratio near two can be obtained.

These results are very disconcerting in view of the need for accuracy in recent and future capture measurements with radioactive beams, and this accuracy does not appear to be available with a stable beam. Therefore, the second purpose of this paper is to test whether an extension of the $A-1$ core to more complicated configurations beyond $0s^3$ can provide theoretical guidance for the ^{4}He(γ,N) reaction. Particular attention is paid to the $\sigma(\gamma,p)/\sigma(\gamma,n)$ ratio because it provides a connection among data sets, and has, in past calculations, shown a large discrepancy between the results of calculations and experiments. In addition, tests are made to see if more complicated core configurations improve nucleon scattering above 60 MeV.

II. THE GENERAL RCCSM

The procedure for the general RCCSM closely follows that of the *p*-shell RCCSM [8]. One picks an oscillator size parameter, $\upsilon=m\omega/\hbar$, which yields a correct fit to the size of the core, and a realistic two-body interaction. The effective interaction may be of any form that is consistent with translational invariance. It may contain central, spin-orbit, quadratic spin-orbit, and tensor terms. The nonspurious $A-1$ core states $|J_A\alpha\rangle$ are then calculated by standard techniques within a specified model space. For $A=4$, this would be the states of ^{3}H and ^{3}He. If one believes that coupling a nucleon onto these core states does not provide a sufficient basis, then additional bound states of the $A=4$ composite system could be calculated. In the notation of Ref. [1], these are noted as beta states $|J_B\beta\rangle$. One must provide the one, two, and three-body densities for the core states,

TABLE I. Oscillator constants, radii and energies.

N	0	2	4	6
υ (fm^{-2})	0.360	0.290	0.315	0.275
^{3}H, $\langle r^2\rangle^{1/2}$ (fm)	1.667	1.669	1.668	1.670
^{3}He $\langle r^2\rangle^{1/2}$ (fm)	1.667	1.721	1.758	1.749
p-separation energy (MeV)	22.5	21.2	20.9	21.3

$$\langle J_A\alpha\|[a^+{}_{k\tau_k}a_{\tau_l}]^{J_x}\|J'_A\alpha'\rangle,$$

$$\langle J_A\alpha\|[(a_k{}^+a_l{}^+)^{J_yT_y}(a_ma_n)^{J_xT_x}]^{JT}{}_{M_T}\|J'_A\alpha'\rangle,$$

and

$$\langle J_A\alpha\|\{[(a_k{}^+a_l{}^+)_\tau{}^{J_xT_x}a^+{}_{l\tau_i}]^{J'_x}[(a_ma_n)_{-\tau}{}^{J_xT_x}a_{p\tau_p}]^{J'_y}\}^J\|J'_A\alpha'\rangle.$$

These quantities are used in calculating the matrix elements of the Hamiltonian, unit operator, and transition operators for *A*-particle system in the shell-model basis. If β states are allowed, then one must provide the overlaps,

$$\langle J_B\beta|[a^+|J_A\alpha\rangle]^{J_B},$$

$$\langle J_B\beta\|[(a_i{}^+a_l{}^+)_{\tau_x}{}^{J_xT_x}a_{k\tau_k}]^J\|J_A\alpha\rangle],$$

and

$$\langle J_B\beta\|\{[(a_k{}^+a_l{}^+)_\tau{}^{J_xT_x}a^+{}_{i\tau_i}]^{j'_x}(a_ma_n)_{-\tau}{}^{J_xT_x}\}^j\|J_A\alpha\rangle.$$

The α states are constructed by coupling one nucleon to the core states in the shell-model coordinate system as, $[a^+{}_{nlj\tau}\otimes|J_A\alpha\rangle]^J$, and the matrix elements of the Hamiltonian,

$$H_A=\sum_{i=1}^{A}p_i{}^2/2m-T_{\text{c.m.}}+\sum_{i<j}^{A}v_{ij}, \tag{1}$$

are calculated in this basis. The present calculations include all $2n+l\leqslant 22$ to insure adequate representation of the wave function within the channel radius. The matrix elements are then transformed to the coordinate connecting the extra nucleon to the center of mass of the core, thus removing spurious components [1]. If β states are included, the matrix elements of the Hamiltonian are calculated among α and β states, and those transformed to the relative coordinate between the center of mass of the core and the last nucleon. The transformation must also be done for the reduced matrix elements of transition operators and for the unit matrix.

To implement the *R*-matrix procedure, the matrix elements are then truncated at a cutoff radius a_c. The unit matrix, **1**, within a_c, is diagonalized to produce an orthogonal basis set, truncated so as not to be overcomplete. One can then set up the standard *R*-matrix equations with this basis as in [22].

III. RESULTS

The procedure to calculate the $E1$ cross section with the *R*-matrix framework is described in Ref. [23] and the references therein. Calculations for the $A=3$ systems are shown below for $N=0$, 2, 4, and 6, where the basis includes all oscillator states with $2(n_1+n_2+n_3)+l_1+l_2+l_3 \leqslant N$, n starts at zero. In each case, an oscillator constant is chosen which reproduces the ^{3}H point charge radius. Comparing calculations with different oscillator constants poses some problems concerning convergence criteria, but it would make no sense to make calculations with an inappropriate core radius. The resulting radii and oscillator constants, along with the proton separation energies are shown in Table I.

Several curves accompany the data for $^4\mathrm{He}(\gamma,p)$ in Fig. 1. The two light-dotted curves with the label $0s^4$ are from calculations with $N=0$, but instead of taking the corresponding RCCSM solution for the ^{4}He ground state, it is taken to be pure $0s^4$ and with the experimental proton separation energy, 19.8 MeV. The two solid, dark-dotted, dashed, and dot-dashed lines are for $N=0$, 2, 4, and 6, respectively. The calculations include only the dominate, spin-independent $E1$ contribution, but the upper set of lines is calculated with the $E1$ current operator, $Q_{10}=2\beta(i/k)p_z(-t_3)$, and the lower set of lines is calculated with the standard Coulomb effective operator, $(Q_{10})_{\mathrm{eff}}=ez(-t_3)$, obtained by applying the continuity equation to the matrix element of $\boldsymbol{p}$. Here, $k=(E_i-E_f)/\hbar c$, $\beta=e\hbar/2mc$, and $t_3(p,n)=\left(-\frac{1}{2},+\frac{1}{2}\right)$. The photon wave number will always be calculated with the theoretical value unless stated otherwise. The upper and lower sets of curves differ by much more than the few percent one would expect from gauge invariant terms or exchange terms. A similar comparison was made in Ref. [24] for the direct capture model. Here it was found that use of the two different transition operators gave vastly different results when the continuum and final state were calculated with different single-particle potentials, but gave nearly the same results when the same potential was used for both.

The difficulty with the two $E1$ transition operators comes in the relation

$$\frac{d}{dt}\langle f|\rho|i\rangle = \frac{i}{\hbar}\langle f|[H,\rho]|i\rangle = -\,\boldsymbol{\nabla}\cdot\langle f|\mathbf{j}|i\rangle. \qquad (2)$$

The Hamiltonian must act left and right, but the initial and final states do not satisfy the operator equation $H\psi=E\psi$. One could use the energies obtained in the model space or one could use the experimental energies, but either way H operating on a model space wave function does not give a constant times the model space wave function. The very same difficulty occurs in $(e,e'p)$ when substituting the density for the third component of the current *via* the continuity equation. One can obtain very different results with the two different operators [6,25]. In conventional distorted wave calculations one has no chance of sorting this out, because the states will never be an eigenfunctions of H, no matter how accurately the residual core state is determined. In contrast, the general RCCSM will provide an accurate solution to the continuum problem and the bound state with the same Hamiltonian, and the only question is whether the basis is big enough. Hence, by calculating the cross sections with both operators, one has a very strict test of the completeness of the basis.

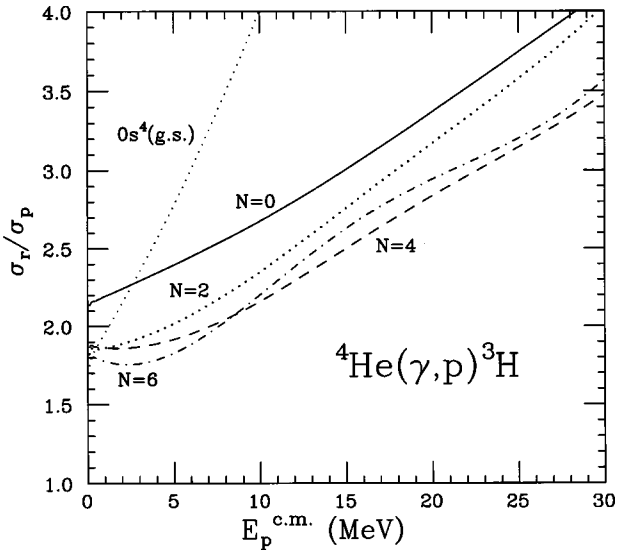

FIG. 3. The ratio of cross sections calculated with Coulomb multipoles to that calculated with transverse current operator. Solid, dark-dotted, dashes, and dot-dashed lines are for $N=0$, 2, 4, and 6, respectively.

For a better comparison between the two operations, the ratios of the cross sections with the Coulomb operator to that with the current operator are plotted in Fig. 3. Graphs using the proton cross sections or neutron cross sections would be indistinguishable to the eye. The light dotted line is again representing the $1p$-$1h$ ($N=0$) calculation with the RCCSM ground state replaced by $0s^4$ and with the experimental proton separation energy. This was the first calculation performed with the RCCSM [3], except that a factor $e^2=1.44$ was erroneously omitted. This curve demonstrates how sensitive the ratio is to having a final state which is a solution to your Hamiltonian, even in a limited basis. The change from the light-dotted line to the $N=0$ solid line is huge. Again questions of convergence with N are clouded by the use of different oscillator constants. In addition, the $N=6$ calculation is having the most difficulty representing the tail of ^{4}He bound state because it is trying to describe a very compact object with oscillator wave functions derived with a large oscillator constant (large b, small v). But the similarity between $N=4$ dashed line and $N=6$ dot-dashes line indicates that one is coming to an end of the improvement that can be obtained by increasing the complexity of the core states. An argument for convergence can also be made from Fig. 1. However, this is actually good news, in that it shows that considerable progress toward current conservation can be

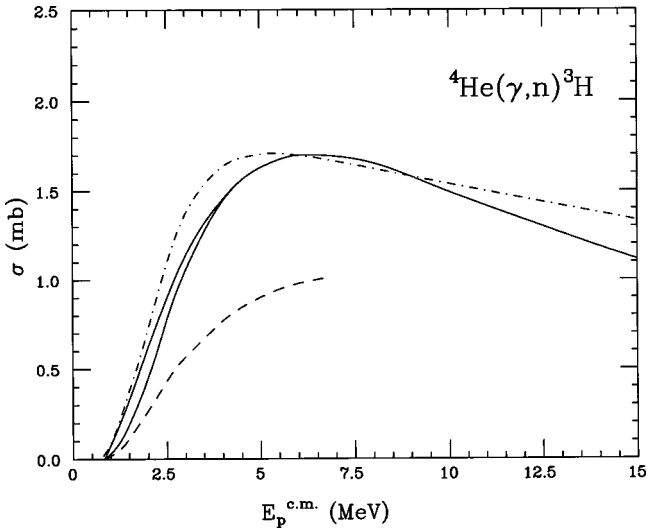

FIG. 4. The ^{4}He$(\gamma,n)^3$H total cross section. Solid lines enclose calculation of Ref. [30], dashed line is from Ref. [32], and dot-dashed line is RCCSM result with effective interaction derived from MTI-III potential.

made by just improving the core state wave functions. Of course this relies on a proper solution of the scattering equations, which would not be possible in distorted wave calculations, where one is not finding a continuum solution to the same Hamiltonian used to generate the bound state wave function.

Returning to Fig. 1, one sees that the decrease in the ratio of operator cross sections is a result of the cross sections from the Coulomb operator becoming smaller and those from the transverse current operator becoming larger. This result is in the correct direction to alleviate the two problems in electron scattering at low momentum transfer as mentioned above.

When the first strong evidence appeared that the ratio of cross sections for ^{4}He$(\gamma,p)^3$H and ^{4}He$(\gamma,n)^3$He were not unity in the energy range, $E_x=20-30$ MeV, [21,26] many attempts were made to reproduce the phenomena within the $1p$-$1h$ version of the RCCSM. All possible multipoles were included, the spin-dependent $E1$ operator was included, the second-order correction to the $E1$, spin-independent operator was included, [23] and the operators were recalculated in Jacobi coordinates in order to eliminate the long-wavelength approximation and correctly calculate the matrix elements of the $1p$-$1h$ contributions of the ^{4}He ground state [6]. Nothing changed the ratio from approximately unity except adding an explicitly charge symmetry breaking interaction [27].

An older calculation in Ref. [28] did produce a ratio of approximately two, but this calculation was essentially a bound state-calculation. However, what it did have were configurations not included in the $1p$-$1h$ RCCSM. The general RCCSM allows one to test the effect of increasing the model space. Only, when one looks at the basis, it could include the deuteron-deuteron channel and three- and four-body breakup. The task would appear daunting. However, the d-d channel and three and four-body breakup were not included in the $1p$-$1h$ model, and still near perfect agreement with nucleon scattering data was obtained. This result plus

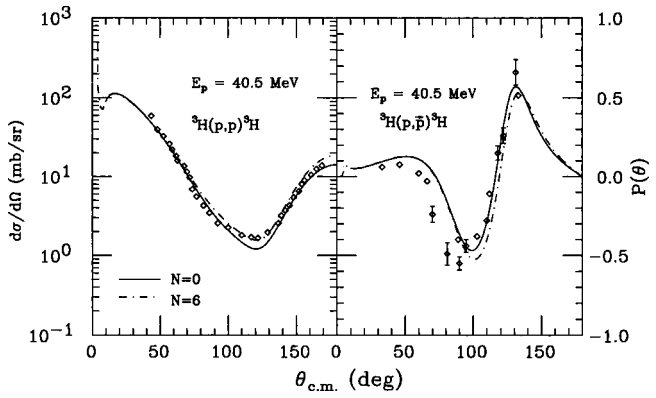

FIG. 5. The 40 MeV cross section and polarization for ^{3}He$(p,p)^3$H. The data are from Ref. [34]. Solid is for $N=0$; dot-dashed line is for $N=6$.

the improvement in the sensitive ratio of cross sections calculated with the transverse current operator and Coulomb operator provide confidence in a calculation with the improved structure in the $A-1$ system. In fact, an improvement in the $A-1$ structure already provides one with a possible source for the $\sigma(\gamma,p)/\sigma(\gamma,n)$ ratio being different from unity. The ^{3}H and ^{3}He radii will not be the same as they were in the $1p$-$1h$ $(N=0)$ model. Shown in Table I in addition to the ^{3}H radii are the calculated ^{3}He r.m.s. radii. This is an asymmetry not tested in previous RCCSM calculations.

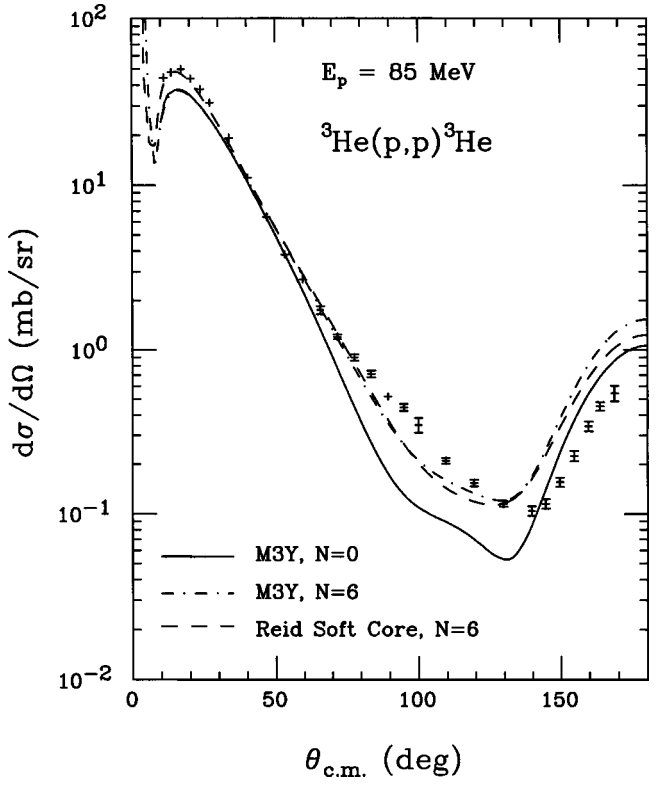

FIG. 6. The 85 MeV cross section for ^{3}He$(p,p)^3$He. Data are from Ref. [35]. Solid line is $N=0$. Dot-dashed line is for $N=6$. Dashed line is for Reid Soft Core g-matrix interaction from Ref. [33].

The $\sigma(\gamma,p)/\sigma(\gamma,n)$ ratio, calculated with the Coulomb operator, for the same five calculations shown in Fig. 1 are shown in Fig. 2. The curves are nearly identical, and the same result is obtained if one uses the transverse current operator. Since the data sets that show the $\sigma(\gamma,p)/\sigma(\gamma,n)$ ratio near two do so by $E_p^{\text{c.m.}}=5$ MeV, and since the ratio of cross sections calculated with the Coulomb operator to that with the transverse current operator is low at that energy, one has a fair degree of confidence in the calculations. Therefore, only those data sets with a ratio near unity at $E_p^{\text{c.m.}}=5$ MeV are acceptable. This includes the data of Refs. [13,16,18] and [19] divided by [21]. Of these, the ones classified as intermediate above provide the best agreement with the magnitude of the $N=6$ result with the Coulomb operator. These would be Refs. [16,18].

The data of Ref. [19] appear to be about 20% low; however, they do fall between the Coulomb and transverse current results. According to Siegert's theorem [29], one has greater confidence in cross sections employing the Coulomb multipole. Use of the experimental proton separation energy in the calculation would lower the curve slightly, and including the $E2$ multipole would increase it slightly, hence, an approximate 20% discrepancy is firm. If the data of Ref. [19] are correct, then this would be another case where the structureless nucleon approximation overestimates a single particle strength.

Although the authors test only the Coulomb $E1$ mutipole, the above results are very similar to those obtained in the recent calculation in Ref. [30]. Here the authors employ the Lorentz integral transform method. The advantage of this method is that it allows calculation of the photodisintegration cross section without the intermediate step of calculating continuum wave functions, and it is an *ab initio* calculation in the sense that they are solving the four-body problem. The disadvantage is that, without the continuum wave functions, one has no other way to test the appropriateness of the solution, such as elastic scattering or charge exchange. In fact, because the central *s*-wave interaction of Malfiet and Tjon [31] (MTI-III) was employed, one is certain that the experimental, low-energy nucleon scattering data will not be reproduced.

The $\sigma(\gamma,p)$ and $\sigma(\gamma,n)$ cross sections obtained by this method are very similar the $N=2$ result of this present work, i.e., slightly higher than the $N=6$ result. However, both the present calculation and that of Ref. [30] produce a shape which is peaked around at $E_p^{\text{c.m.}}=6$ MeV and a $\sigma(\gamma,p)/\sigma(\gamma,n)$ ratio near unity. The shape of the $\sigma(\gamma,n)$ cross section obtained in this present work and that of Ref. [30] differs from that in Ref. [32], where the Alt-Grassberger-Sandhas integral equations were solved. This is a bit surprising since the MTI-III potential was also employed as in Ref. [30] and both solve the four-body problem, albeit by different methods. The $\sigma(\gamma,n)$ cross section of Ref. [32] is flatter in the peak region and resembles the data of Ref. [21].

Although the RCCSM is not an *ab initio* calculation, one can obtain an effective interaction from the MTI-III potential and determine whether a subsequent calculation for the $\sigma(\gamma,n)$ resembles that of Refs. [30] or [32]. One follows a procedure similar to that used to generate the effective interaction from the Reid potential used below [33]. Perform a Brueckner calculation for ^{4}He with $v=0.36$ fm^{-2} and a propagator, $\omega-(H_{\text{osc}}-\Delta)$. Fit the resulting hole-hole and particle-hole, two-body matrix elements to sums of Yukawas to produce an effective interaction. Calculate the ^{2}H, ^{3}H, ^{3}He, and ^{4}He binding energies within the 0*s* model space. Vary Δ until the binding energies closely reproduce those from exact calculations. With $\Delta=30$ MeV, binding energies of 2.22, 8.57, 7.88, and 28.35 MeV are obtained. An $N=0$ calculation is then performed since that keeps ^{3}H and ^{3}He in the 0*s* model space. The resulting cross section is shown as a dot-dashed line in Fig. 4 along with the calculation of Ref. [30] as lying within the two solid lines and the calculation of Ref. [32] as a dashed line. The present calculation appears to more closely resemble that of Ref. [30].

As mentioned above, the cross sections from the $1p$-$1h$ calculations for nucleon scattering begin to vary from the experimental cross sections at about 60 MeV. To illustrate this effect, the 40.5 MeV cross section and polarization for $^3\text{H}(p,p)^3\text{H}$ are plotted in Fig. 5 for $N=0$ as a solid line and $N=6$ as a dot-dashed line along with the data of Ref. [34]. The agreement is good, and the difference between the $N=0$ and $N=6$ calculations is minimal. Here it would appear that the cross sections are insensitive to the structure.

In Fig. 6 is plotted the $N=0$ result as a solid line for $^3\text{He}(p,p)^3\text{He}$ at 85 MeV, and one sees the disagreement with the data of Ref. [35] developing around 120°. The question that arises is whether the disagreement is due to the simple $N=0$ structure or the effective interaction. The dot-dashed line is the $N=6$ result. It differs little from the $N=4$ result. The minimum begins to fill in nicely, but the back-angle rise increases. Also, the minimum is not at quite the correct angle. One could argue that the $N=6$ result is an improvement since nucleon knockout, omitted from the calculation, would reduce the back-angle cross section. However, the forward angle cross section remains small. This can be cured, as seen in the dashed line, by using the ^{4}He effective interaction described in Ref. [33] and derived from the Reid Soft Core potential. This effective interaction is very similar to M3Y, since most of the matrix elements used to construct M3Y were Reid Soft Core *g*-matrix elements. The interaction gives low energy results that are almost as good as M3Y, and as seen here, gives better medium energy results. So part of the disagreement with the 85 MeV cross section was due to structure and part due to the effective interaction. One could argue, however, that it was not the structure, but the better ^{3}He density distribution of $N=6$ that produced a better cross section. Within the RCCSM, one could not separate the two.

IV. CONCLUSION

This article has introduced a general RCCSM which allows inclusion of any $A-1$ shell-model core states, as long as they are nonspurious, and any states of the composite system, as long as they are nonspurious, and include them in a calculation with one nucleon in the continuum. The model demonstrated that increasing the model space of the $A=3$ core from $0\hbar\omega$ to $6\hbar\omega$ decreases the $^4\text{He}(\gamma,p)^3\text{H}$ cross sec-

tion calculated with a Coulomb operator and increases that calculated with the transverse current operator, hence, improving current conservation. An increased model space did not, however produce a $\sigma(\gamma,p)/\sigma(\gamma,n)$ ratio different from unity. This result favors the data of Refs. [16] and [18]. An improvement was seen in the ^{3}He$(p,p)^3$He cross section at 85 MeV as the $N=6$ results filled in the midangle cross section. However, agreement at the forward angles required changing form the M3Y interaction to one entirely based on the Reid Soft Core potential.

ACKNOWLEDGMENT

This work was supported by the National Science Foundation under Grant No. PHY-0099452.

[1] R. J. Philpott, Nucl. Phys. **A289**, 109 (1977).
[2] D. Halderson and V. A. Sadovnikova, Phys. Rev. C **56**, 2688 (1997).
[3] D. Halderson and R. J. Philpott, Nucl. Phys. **A321**, 295 (1979).
[4] R. J. Philpott and D. Halderson, in *The* (p,n) *Reaction and the Nucleon-Nucleon Force*, edited by C. D. Goodman, S. M. Austin, S. D. Bloom, J. Rapaport, and G. R. Satchler (Plenum, New York, 1980), p. 491.
[5] D. Halderson and R.J. Philpott, Nucl. Phys. **A359**, 365 (1981).
[6] D. Halderson, Phys. Rev. C **53**, 2978 (1996).
[7] D. Halderson, R. J. Philpott, J. A. Carr, and F. Petrovich, Phys. Rev. C **24**, 1095 (1981).
[8] D. Halderson, Nucl. Phys. **A707**, 65 (2002).
[9] D. Halderson, Phys. Rev. C **69**, 014609 (2004).
[10] G. Bertsch, J. Borysowicz, H. McManus, and W. G. Love, Nucl. Phys. **A284**, 399 (1977), the interaction described on p. 412.
[11] W. G. Meyerhoff, M. Suffert, and W. Feldman, Nucl. Phys. **A148**, 211 (1970).
[12] J. R. Calarco, S. S. Hanna, C. C. Chang, E. M. Diener, E. Kuhlman, and G. A. Fisher, Phys. Rev. C **28**, 483 (1983).
[13] A. N. Gorbunov, Phys. Lett. **27B**, 436 (1968); Proc. of P. N. Lebedev Phys. Inst. **71**, 1 (1974).
[14] L. Van Hoorebeke, R. Van de Vyver, V. Fiermans, D. Ryckbosch, C. Van den beele, and J. Dias, Phys. Rev. C **48**, 2510 (1993).
[15] A. N. Horbunov, Phys. Lett. **27B**, 436 (1968); Zh. Eksp. Teor. Fiz. Pis'ma Red. **8**, 148 (1968) [JETP Lett. **8**, 188 (1968)].
[16] F. Balestra, E. Bollini, L. Busso, R. Garfagnini, C. Guaraldo, G. Piragino, R. Scrimaglio, and A. Zanini, Nuovo Cimento Soc. Ital. Fis., A **38**, 145 (1977).
[17] Yu. M. Arkatov, P. I. Vatset, V. I. Voloshchuk, V. V. Kirichenko, I. M. Prokhorets, and A. F. Khodyachikh, Yad. Fiz. **12**, 227 (1970) [Sov. J. Nucl. Phys. **12**, 123 (1971)].
[18] W. R. Dodge and J. J. Murphy II, Phys. Rev. Lett. **28**, 839 (1972).
[19] G. Feldman, M. J. Balbes, L. H. Kramer, J. Z. Williams, and H. R. Weller, Phys. Rev. C **42**, R1167 (1990).
[20] R. Bernabei, A. Chisholm, S. d'Angelo, M. P. DePascale, P. Picozza, C. Schaerf, P. Belli, L. Casano, A. Incicchitti, D. Prosperi, and B. Girolami, Phys. Rev. C **38**, 1990 (1988).
[21] L. Ward, D. R. Tilley, D. M. Skopik, N. R. Roberson, and H. R. Weller, Phys. Rev. C **24**, 317 (1981).
[22] R. J. Philpot, Nucl. Phys. **A243**, 260 (1975).
[23] D. Halderson and R. J. Philpott, Nucl. Phys. **A359**, 365 (1981).
[24] J. M. Lafferty, Jr. and S. R. Cotanch, Nucl. Phys. **A373**, 363 (1982).
[25] J. E. Amaro, B. Ameziane, and A. M. Lallena, Phys. Rev. C **53**, 1430 (1996).
[26] B. L. Berman, D. D. Faul, P. Meyer, and D. L. Olson, Phys. Rev. C **22**, 2273 (1980).
[27] D. Halderson and R. J. Philpott, Phys. Rev. C **28**, 1000 (1983).
[28] B. F. Gibson, Nucl. Phys. **A195**, 449 (1972).
[29] A. J. F. Seigert, Phys. Rev. **52**, 787 (1937).
[30] S. Quaglioni, W. Leidemann, G. Orlandini, N. Barnea, and V. D. Efros, Phys. Rev. C **69**, 044004 (2004).
[31] R. A. Malfliet and J. Tjon, Nucl. Phys. **A127**, 161 (1969).
[32] G. Ellerkmann, W. Sandhas, S. A. Sofianos, and H. Fiedeldey, Phys. Rev. C **46**, 449 (1992).
[33] D. Halderson, J. Phys. G **20**, 1461 (1994).
[34] R. Darves-Blanc, Van Sen Nguyen, J. Arvieus, A. Fiore, J. C. Gondrand, and G. Perrin, Lett. Nuovo Cimento Soc. Ital. Fis. **4**, 16 (1972).
[35] L. G. Votta, P. G. Roos, N. S. Chant, and R. Woody III, Phys. Rev. C **10**, 520 (1974).